Microchimica Acta (2020) 187:320
https://doi.org/10.1007/s00604-020-04286-8

ORIGINAL PAPER

Amperometric immunosensor based on covalent organic frameworks and Pt/Ru/C nanoparticles for the quantification of C-reactive protein

Ting-Zhi Liu[1] · Rong Hu[1] · Yi Liu[1] · Kun-Lei Zhang[1] · Ru-Yan Bai[1] · Yun-Hui Yang[1]

Received: 11 December 2019 / Accepted: 19 April 2020

Abstract

An ultrasensitive and nonenzymatic electrochemical sandwich-type immunoassay using covalent organic framework (COF-LZU1) material applied as a fixed matrix was developed for the determination of C-reactive protein (CRP). COFs with large specific surface area, good conductivity and stability were employed for functionalisation of the surface. Au nanoparticles were loaded on COF-LZUl to immobilise the CRP antibody (anti-CRP) on the surface of a glassy carbon electrode. Microwave method was employed for the synthesis of the Pt/Ru/C nanoparticles to imitate the protein enzyme with high catalytic activity. The as-synthesised activated carbon–supported bimetallic Pt/Ru/C nanoparticle composite was used to label secondary CRP antibody because it exhibited excellent catalytic behaviour toward hydrogen peroxide. After incubation of CRP, Pt/Ru/C-labelled anti-CRP was combined with CRP through specific antibody-antigen recognition process. The reduction current of H_20_2 at − 0.2 V catalysing by tag Pt/Ru/C as measured by a chronoamperometric method is proportional to the concentration of CRP. Under optimal experimental conditions, employing chronoamperometry to investigate the CRP, the obtained linear range was 0.2 to 20 ng/mL with a detection limit of 0.1 ng/mL. This immunosensor provides an attractive platform for the applicability of COF-LZU1 materials and Pt/Ru/C nanoparticles in electrochemical assays.

Keywords Covalent organic frameworks (COF-LZU1) · Pt/Ru/C nanoparticles · C-reactive protein (CRP) · Nonenzymatic immunosensor

Introduction

C-reactive protein (CRP) is a biomarker of clinically acute and chronic inflammation, which is one of the acute phase proteins in healthy blood, while the amount of CRP can sharply increase when the bodies got injured and burned or other varieties of health issues are appearing, including liver disease, infection, chronic inflammation and cancer [1–3]. In the clinical investigations, CRP is useful and could provide information for the calculation of the risk of Framingham at all levels and the prognostic information of the metabolic syndrome. Moreover, the high concentrations of CRP can have a close relationship with cardiovascular disease [4, 5], being one of the most potent predictive factors for this group of diseases [6, 7]. The utilization of the electrochemical method is one of the most attractive techniques for target determination due to its intrinsic sensitivity and low cost, at the same time simple and portable [8–11]. To increase the sensitivity, native enzymes, e.g. horseradish peroxidase (HRP), were usually employed. However, the limited stability of the immobilised enzymes and their native conformations will be easily disrupted, losing their catalytic activity.

Recently, a large number of nanomaterials, such as carbon nanomaterials have been synthesised to resolve these issues, increasing the ability of electron transfer and their excellent catalytic behaviours toward small molecules, such as hydrogen peroxide (H_2O_2), dopamine and ascorbic acid [12–14]. Those nanomaterials can owe an intrinsic enzyme-mimicking activity similar to that of natural HRP, while,

Electronic supplementary material The online version of this article (https://doi.org/10.1007/s00604-020-04286-8) contains supplementary material, which is available to authorized users.

✉ Rong Hu
hudierong_168@163.com

✉ Yun-Hui Yang
yyhui2002@aliyun.com

[1] College of Chemistry and Chemical Engineering, Yunnan Normal University, Kunming 650092, Yunnan, People's Republic of China

Published online: 12 May 2020

compared with the enzyme, they are more stable. Therefore, it is a critical demand for simple, rapid, sensitive, stable and low-cost detection technologies for fast and sensitive profiling of CRP based on nanomaterials, especially in the point-of-care applications.

Activated carbon is a porous and low-cost carbonaceous material [15–17], which became one of the most popular materials in many research areas, due to their large specific surface area, high chemical stability and catalytic properties, especially in single-atom catalysts [18, 19]. It is already reported that a metal core coated with a carbon shell can simultaneously promote the catalytic activity through the synergism and enhance the stability due to the protection from carbon cage (C) [20, 21]. In particular, in the case of carbon nanomaterials with bimetallic nanocomposites, the synergy effect of the two metals makes its own better electrical, catalytic and magnetic properties than in the case of single-metal-based nanostructures [22, 23]. For example, Nanda et al. reported Pd-coated Ru nanocrystals supported on N-doped graphene for hydrogen evolution reaction, showing that the catalytic ability of bimetallic alloy is much better than those values obtained for Pd/C or Ru/C [24]. Li et al. synthesised AuPd nanocluster as a peroxidase mimic and prepared an assay for the detection of acid phosphatase [12]. In the biosensor field, these metal-supported carbon nanoparticles with high catalytic activity not only could work as a promoter to increase the surface area and to improve the electron transfer at the surface of the electrode, but also could be employed as carriers to load more amount of labels and biomolecules. Therefore, it can be interesting to investigate activated carbon–supported bimetallic nanoparticle composites which can owe better catalytic efficiency toward CRP determination, especially in the point-of-care applications.

Covalent organic frameworks (COFs) are a unique class of crystalline porous architectures with high surface area and a relatively stable structure because of their layered-sheet arrangement with an open channel and high charge carrier mobility [25, 26]. As a relatively new type of material, COFs can have two- or three-dimensional crystalline structures with high structural regularity, large specific surface areas and excellent conductivity, which are advantageous toward an increased efficiency of electron transfer in the materials [25, 26]. Since the first discovery of COF materials in 2005 by Yaghi et al. [27], this topic has attracted broad interest from researchers in materials science, due to their applicability in gas storage [28], semiconductors [26], optoelectronic devices [29] and catalysis [30]. For example, Wang et al. reported the application of COFs materials, a Pd (II)–containing COF (Pd/COF-LZU1), for highly efficient catalysis [30]. On the other hand, Banerjee et al. reported "turn-on" detection capability for 2,4,6-trinitrophenol (TNP) of the COFs in the solid state [31]. In the framework of these investigations, our group reported a novel and simple electrochemical immunoassay based on Pt-COFs [32]. Because COFs have a large specific surface area, good conductivity, excellent stability and the advantages of a more accessible surface for functionalisation, it is highly beneficial to construct novel electrochemical systems based on COFs for determination of CRP, allowing high electronic conductivity and low detection limits.

Taking into account the aspects mentioned above, the present work aimed to develop C-reactive protein immunosensor based on the covalent organic frameworks (COF-LZU1) material (Scheme 1). Because Au nanoparticles are easy to combine with the antigen-antibody, in the present article, Au nanoparticles were loaded on the surface of COF-LZUl in order to synthesise functional COFs material (Au/COF-LZUl) for the preparation of electrochemical assay. CRP antibodies were immobilised onto the surface of a glassy carbon electrode through the porous structure of covalent organic framework materials between Au nanoparticles and -SH of antibody. In this work, for the first time, microwave heating method was used to in situ synthesise Pt/Ru/C nanocomposites, which can have an increased catalytic effect on the reduction of H_2O_2 compared with the monometallic Pt/C or Ru/C nanocomposites. Furthermore, Pt/Ru/C nanocomposites were used to label anti-CRP instead of using enzymes for preparing sandwich-type electrochemical immunosensors for the determination of CRP. In comparison with natural enzymes, Pt/Ru/C NPs show superior thermal stability along with higher pH tolerance. The proposed immunosensor has low detection limits due to the high electronic conductivity of Au/COF-LZUl and the excellent catalytic effect of Pt/Ru/C nanocomposites.

Experimental

Reagents and chemicals

Chloroauric acid ($HAuCl_4 \cdot 4H_2O$) and chloroplatinic acid (H_2PtCl_6) were purchased from Kunming Boren Precious Metals Co. Ltd. (Kunming, China); XC-72R activated carbon was obtained from Shanghai Cabot Corp. (Shanghai, China); potassium hydroxide was acquired from Beijing Chemworks (Beijing, China); trisodium citrate dihydrate ($Na_3C_6H_5O_7 \cdot 2H_2O$), ethylene glycol and ethyl alcohol absolute were purchased from Tianjin Fengchuan Chemical Reagent Technologies Co., Ltd. (Tianjin, China); C-reactive protein monoclonal (CRP) antibodies (anti-CRP, the antibody titer 1.6×10^{-10} moL) and CRP were bought from Shanghai Linc-Bio Science Co. Ltd. (Shanghai, China); ruthenium (III) chloride hydrate ($RuCl_3 \cdot xH_2O$) was purchased from Shanghai SiYu Co. Ltd. (Shanghai, China); 30% H_2O_2, tetrahydrofuran (THF) and DMF were purchased from Xilong Chemical Co. Ltd. (Beijing, China); chitosan (CHIT), glutaraldehyde (GA), bovine serum albumin (BSA), 1,4-diaminobenzene and 1,4-dioxane and phosphate buffer saline

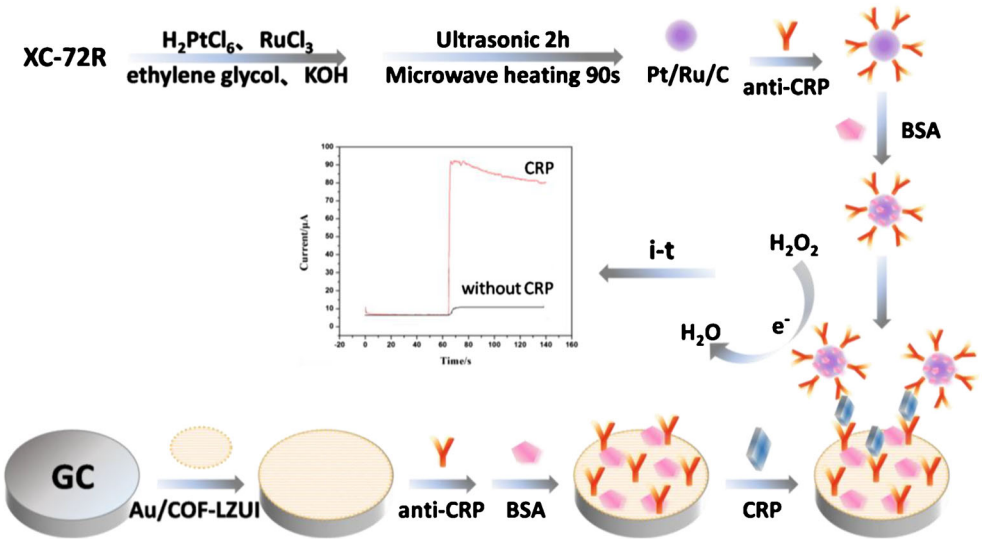

Scheme 1 Stepwise procedure of the immunosensor

(PBS, 0.01 mol/L phosphate, 0.138 mol/L NaCl, pH 7.4) were acquired from Sigma-Aldrich Co. Ltd. (American); acetic acid was purchased from Chengdu Chemical Reagent (Chengdu, China); and 1,3,5-triformylbenzene was obtained from J & K Technology Co. Ltd. All reagents used in the experiment were analytical reagents, and the water used in experiments was redistilled.

Apparatus

Cyclic voltammetry, electrochemical impedance and amperometric measurements were carried out using a CHI 660D electrochemical workstation (Shanghai CH Instruments Co., China). A three-electrode cell was used with a modified glassy carbon electrode (GCE) as the working electrode, a saturated calomel electrode (SCE) as a reference electrode and a platinum foil electrode as an auxiliary electrode. All potentials were measured and reported vs the used SCE. Transmission electron microscopy (TEM) analysis was performed using a JEM-2100 microscope (Japan) at 200KV.

Synthesis of materials

Pretreatment of the carbon carrier

100 mg XC-72R activated carbon was dispersed in concentrated HNO_3 (15 mL) and heated at reflux for 4 h. After cooling down to the room temperature, the above suspension was filtered, washed with redistilled water for three times, placed in a vacuum oven to dry for use finally.

Preparation of the Au/COFs materials

Covalent organic framework materials (COF-LZUl) were prepared according to the literature [30]. Briefly, 0.16 g (15 mmol) of 1,4-diaminobenzene and 0.16 g (10 mmol) of 1,3,5-triformylbenzene were placed on the reaction tube. Then, 10.0 mL of 1,4-dioxane was added in order to dissolve the solid mixture. Afterwards, 2.0 mL of 3 mol L^{-1} acetic acid was dropped to the tube slowly. With the dropping of the acetic acid, a yellow solid phase was obtained, and the tube was placed in the vacuum. Next, the tube was transferred to the drying oven for 3 days at 120 °C. After cooling down to the room temperature, THF was placed in the tube and followed with centrifuging and washing with DMF and THF, respectively. Then, the resulting solid was washed with THF using Soxhlet extraction for 24 h and then dried at 80 °C under vacuum for 12 h. In the last step, a yellow powder was obtained, which was the COFs.

In order to obtain the Au NP–based composite, 50 mg of COFs was ultrasonically dispersed in 50.0 mL of H_2O for 30 min. Then, 1.0 mL 1% $HAuCl_4$ was added to the ultrasonic dispersion. After 1 h, the mixture was heated at reflux to 90 °C, and 3.5 mL of 1% sodium citrate solution was added quickly, and the reaction mixture was refluxed continuously for 12 h. The as-obtained solution was centrifuged (relative centrifugal force, RCF = 8000), washed with the deionised water and finally resuspended in deionised water to preserve for use.

Microwave synthesis of Pt/Ru/C catalyst nanomaterials

$H_2PtCl_6 \cdot 6H_2O$ and $RuCl_3 \cdot xH_2O$ were used to synthesise the Pt/Ru/C catalyst. Briefly, 25.0 mL of ethylene glycol, 1.0 mL of 0.05 mol L^{-1} $H_2PtCl_6 \cdot 6H_2O$, 1.0 mL of 0.05 mol L^{-1} $RuCl_3 \cdot xH_2O$ solution, 0.5 mL of 0.40 mol L^{-1} KOH solution and 0.040 g XC-72R activated carbon were added to a 100-mL beaker in turn and ultrasonically dispersed for 2 h. After the successful dispersion, the beaker was placed in the microwave oven to heat for 90 s. Then, the as-obtained

solution was centrifuged (RCF = 10,000) and washed with acetone and deionised water. In the last step, the precipitate was resuspended in 4 mL of deionised water.

Labelling Pt/Ru/C nanomaterials on anti-CRP

The amount of the 200 mmol L^{-1} Na_2CO_3 was added to the 1 mL of concentrated Pt/Ru/C nanomaterial to adjust pH to 9. Then, 10 μL of 1 mg/mL CRP antibody was pipetted to the mixed solution by five times, and each interval was 3 min. After the solution was left to stand overnight at 4 °C, 25 μL of BSA (1%) was added to the solution to block nonspecific binding sites for half of an hour. In the last step, the as-obtained solution was centrifuged (RCF = 6000) at a low temperature (12.0 °C) for 15 min. The precipitate was washed with PBS for two times and resuspended in 4 mL eluent buffer and kept at 4 °C until utilisation.

Fabrication of the anti-CRP immunosensor

A GC electrode (Φ = 3 mm) was firstly polished with metallographic sandpaper, followed by three particle sizes (1.0, 0.3 and 0.05 μm) of alumina to obtain a mirror-like surface, being ultrasonically cleaned afterwards with a mixture of nitric acid (1:1) and absolute ethanol and redistilled water for 10 min, in turn, to remove the physically adsorbed substances and the as-cleaned electrode was allowed to dry at room temperature. A solution was obtained by ultrasonic mixing of 10 μL of 0.5% CHIT and 10 μL of Au/COFs and a drop of 10 μL of the mixed solution was pipetted on a cleaned electrode surface. After drying, the electrode was washed with PBS buffer for three times. Following this, 10 μL of 10 μg/mL of CRP antibody was dropped and dried overnight at 4 °C. Then, the modified electrode was washed with sterile PBS and was incubated in 10.0 μL 1% BSA for 1 h at 37 °C to block the remaining active groups and eliminate the nonspecific binding effect. After blocking the active groups on the surface, the electrode was washed with PBS for three times and dried naturally. The modified electrode was used finally for the determination of CRP.

Electrochemical determination of CRP

Before determination, the immunosensor was incubated with different concentrations of CRP solutions for 50 min at 37 °C, followed by rinsing thoroughly with PBS and dried. Then, the immunosensor was incubated with 10 μL of Pt/Ru/C-labelled anti-CRP for 45 min at 37 °C. Afterwards, it was rewashed with PBS. Regarding the immunosensor as the working electrode, 10 mL of 0.01 mol/L PBS was added to 100 μL of 1 mol/L H_2O_2 for chronoamperometry determination at − 0.2 V to realise the quantitative detection of CRP. The stepwise procedure of the construction of immunosensor was shown in Scheme 1.

Results and discussion

Choice of label materials

Carbon nanomaterials are low-cost and high electron-transfer material, such as carbon nanotube and graphene, which became one of the most popular materials in many research areas. These carbon nanomaterials have high catalytic behaviours toward H_2O_2. However, carbon nanotubes are unsoluble. Graphene with its insulating property is not easy to label on the antibody [32]. According to the literature, in the case of carbon nanomaterials with bimetallic nanocomposites, the synergy effect of the two metals makes its own better electrical, catalytic and magnetic properties than in the case of single-metal-based nanostructures [22, 23]. Here, we investigate activated carbon–supported bimetallic nanoparticle composites (Pt/Ru/C) to see whether it can be used as a label owing better catalytic efficiency than Pt/C and Ru/C toward the reduction of H_2O_2 to construct CRP immunosensor. 10 μL of different nanomaterial (Pt/Ru/C, Pt/C and Ru/C, respectively)–labelled antibodies and 10 μL of chitosan solution were mixed to modify the bare GCE. After drying, the GCE was immersed in support electrolyte (PBS), and 100 μL of 1 mol/L H_2O_2 was added to the PBS for determination of the current by chronoamperometry at − 0.2 V. The results were shown in Fig. 1. Curves a, b and c represents the catalytic current response of different nanomaterial (Pt/Ru/C; Pt/C; Ru/C)–labelled anti-CRPs

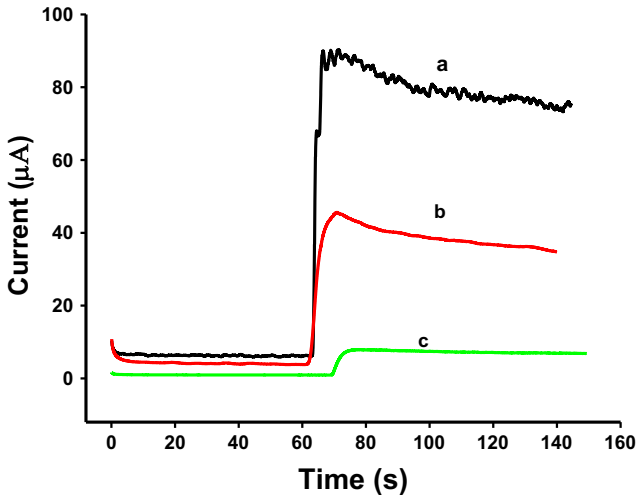

Fig. 1 The catalytic effect of different nanomaterial-labelled anti-CRP modified electrodes to the reduction of H_2O_2 at − 0.2 V ((a) Pt/Ru/C-labelled anti-CRP/GCE; (b) Pt/C-labelled anti-CRP/GCE; (c) Ru/C-labelled anti-CRP/GCE)

toward H_2O_2. As can be observed, both Pt and Ru with carbon material as supporting matrix have good catalytic effect on the reduction of H_2O_2. However, when the labelled nanomaterials were Pt/Ru/C, the catalytic efficiency toward H_2O_2 was maximised and could produce a strong current response signal, which could prove the synergistic catalytic effect of the components in Pt/Ru/C. Moreover, Pt/Ru/C NPs with small size could be dispersed in water very well and labelled on anti-CRP. Therefore, Pt/Ru/C nanomaterials were chosen as label materials in further experiments.

Characterisation of COFs and Au/COFs nanomaterials

The morphologies of COF-LZUl and Au/COFs-LZUl (Fig. 2) were obtained with different magnifications by scanning electron microscopy (SEM) and TEM. The SEM image of COF-LZU1 (Fig. 2(a)) shows the layered-sheet morphology of the sample, while the boundaries of the TEM micrographs (Fig. 2(b)) are also showing the above-mentioned layered-sheet arrangement of COF-LZU1 with an average size of 200 nm. The X-ray diffraction (XRD) data shows that the as-prepared COF-LZU1 owns a characteristic diffraction peak around 5°, attributing to the (100) diffraction (Fig. S1) [30]. From Fig. 2(c, d), it can be observed that Au NPs were distributed on the surface of COF-LZU1. These results demonstrate that the COF-LZUl and Au/COF-LZUl were obtained successfully.

Characterisation of the Pt/Ru/C nanomaterials

XC-72R and Pt/Ru/C nanomaterials were ultrasonically dispersed in ethanol and characterised by TEM. From the as-obtained micrographs, it can be observed that the size of the XC-72R nanostructures was about 80 nm (Fig. 3(a)). The high-resolution transmission electron microscopy (HRTEM) image of XC-72R displays a well-resolved lattice fringe spacing with interplanar distances (Fig. 3(b)). The TEM image of the Pt/Ru/C nanoparticles is shown in Fig. 3(c) and (d). It can be observed that a large number of darker dots are distributed, showing that Pt and Ru were on the surfaces of XC-72R (Fig. 3(c, d)). The energy spectrum of Pt/Ru/C nanospheres was also investigated in Fig. 3(e). From the energy spectrum of Pt/Ru/C NPs, the analysis of the Pt/Ru/C bimetallic nanoparticles demonstrated that the as-synthesised nanomaterials in this experiment were Pt/Ru/C NPs. The above results demonstrate that the XC-72R and Pt/Ru/C NPs were successfully obtained.

Cyclic voltammetric characterisation

The cyclic voltammogram of Pt/Ru/C/GCE was recorded between − 0.6 and + 0.3 V using a scan rate of 100 mV/s. Figure S2 in Electronic Supporting Material shows the cyclic voltammograms obtained with the Pt/Ru/C/GCE in unstirring 0.01 M PBS (pH 7.4) without H_2O_2 (a) and with 10 mmol/L

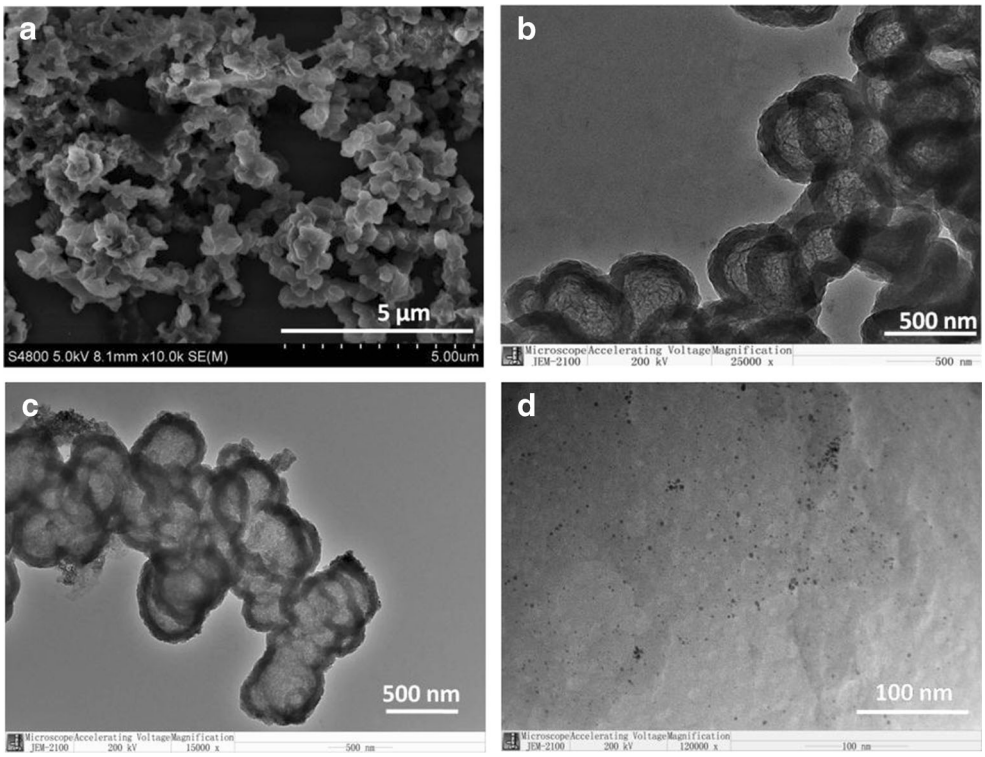

Fig. 2 The SEM images of COF-LZU1 (a); TEM images of COF-LZUl (b) and Au/COF-LZUl (c, d); a magnification figure for Au/COF-LZUl (d)

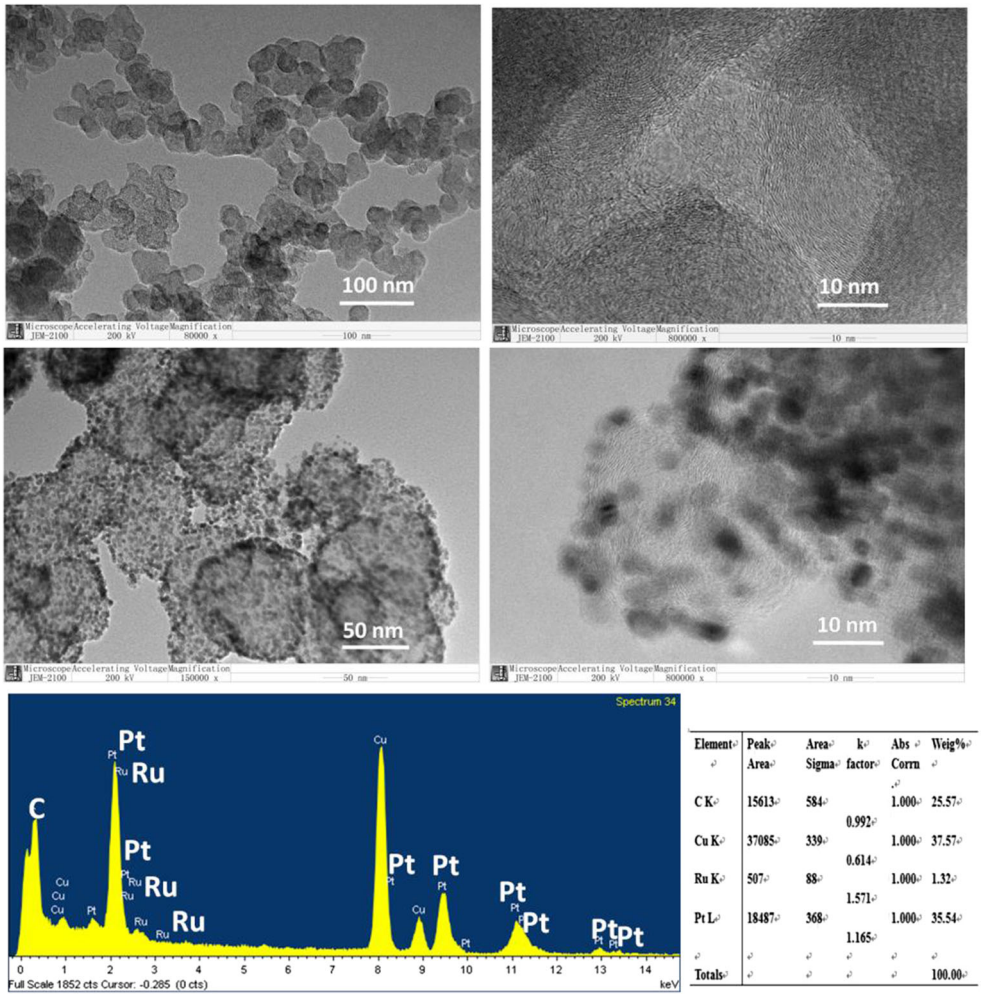

Element	Peak Area	Area Sigma	k factor	Abs Corrn	Weig%
C K	15613	584	0.992	1.000	25.57
Cu K	37085	339	0.614	1.000	37.57
Ru K	507	88	1.571	1.000	1.32
Pt L	18487	368	1.165	1.000	35.54
Totals					100.00

Fig. 3 The TEM illustration of the XC-72R (a) and the HRTEM image of XC-72R (b); (c, d) the TEM image of Pt/Ru/C; (e) EDS analysis of the Pt/Ru/C bimetallic nanoparticles surface of Cu screens

H_2O_2 added (b). No oxidation and reduction peaks were observed (Fig.S2 (a)). In the presence of 10 mmol/L H_2O_2 (Fig. S2 (b)), the cathode peak current at − 0.38 V increased, indicating the reduction of H_2O_2 was catalysed by Pt/Ru/C. To avoid interfering with reducing substances such as ascorbic acid, − 0.2 V was chosen as the applied potential to determine the reduction current of H_2O_2 catalysed by label Pt/Ru/C in a subsequent experiment.

Electrochemical impedance spectroscopy of different modified electrodes

Figure 4 shows the results of electrochemical impedance spectroscopy (EIS) for differently modified electrodes in the solution of 5 mmol L^{-1} of $K_3Fe(CN)_6/K_4Fe(CN)_6$. The bare GCE displayed a minimal impedance (curve a, $R_{et} = 200\ \Omega$), demonstrating the diffusion controlling the electron transfer. A slight change of the electrochemical impedance occurred after GCE was modified with Au-COFs by chitosan (curve b) because COFs with periodic arrays of π clouds owned high electronic conductivity ($R_{et} = 100\ \Omega$). After immobilising anti-CRP on the surface of Au-COFs/GCE, the interfacial resistance value (curve c) was bigger than the previous one

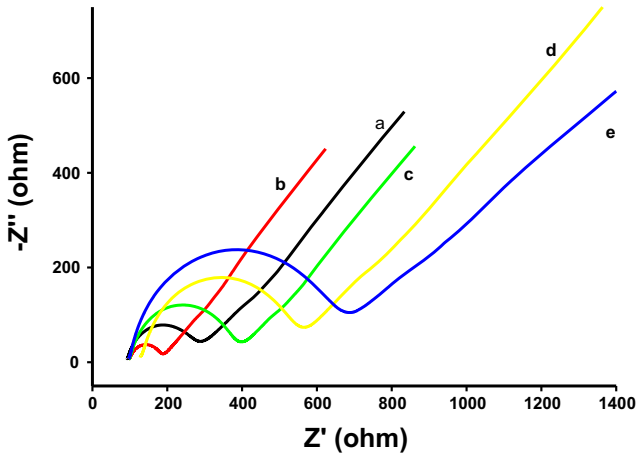

Fig. 4 Electrochemical impedance spectroscopy by using different modified electrodes in 5 mmol/L $[Fe(CN)_6]^{3-/4-}$ ((a) bare GCE; (b) Au-COFs/GCE; (c) anti-CRP/Au-COFs/GCE; (d) CRP/anti-CRP/Au-COFs/GCE; (e) Pt/Ru/C-labelled anti-CRP/CRP/anti-CRP/Au-COFs/GCE). Initial potential (V) 0.155; high frequency (Hz) 100,000; low frequency (Hz) 0.1; amplitude (V) 0.005; quiet times (s) 2

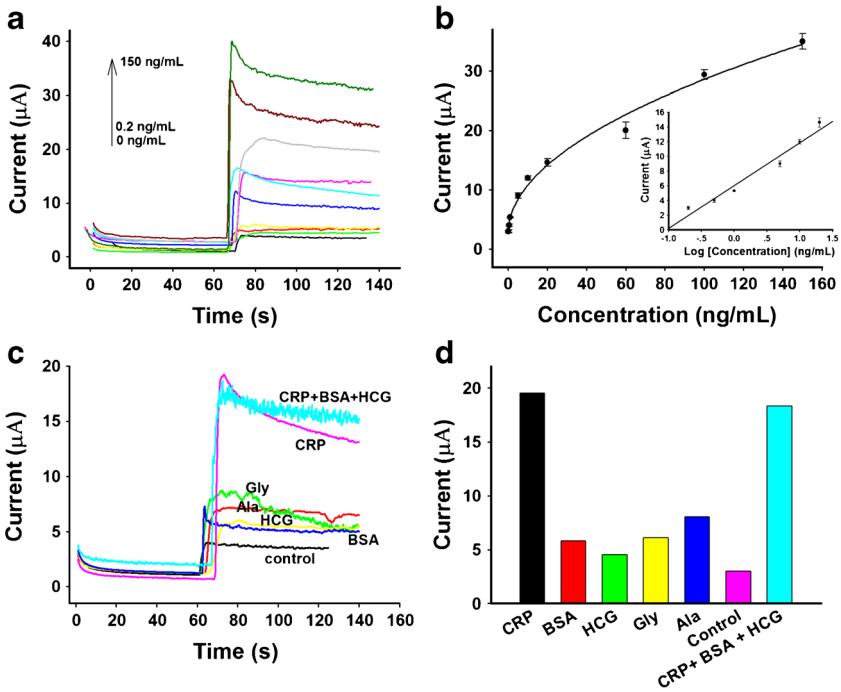

Fig. 5 (a) Typical *I*–*t* curves of the assay in response to CRP of varying concentrations. (b) The relationship of the response current with the increase of concentration of CRP; insert are a relationship of the response current with the logarithm of the low concentration of CRP. (c, d) Selectivity of the CRP electrochemical immunosensors. The chronoamperometry determination was applied at − 0.2 V

(R_{et} = 400 Ω). Because the non-conductivity of the antibody blocked the transfer of the electrons, this indicates that the antibody was successfully immobilised on the surface of the electrode. In the next step, the anti-CRP/Au-COFs/GCE was blocked with BSA and was further incubated with CRP. The value of resistance increased sharply (curve d), because of the cover of BSA and the specific binding of the antibody and antigen blocked the electron transfer (R_{et} = 570 Ω). After the CRP/anti-CRP/Au-COFs/GCE was incubated with Pt/Ru/C nanomaterials labelled anti-CRP, the resistance value increased further (R_{et} = 700 Ω), which indicates that the Pt/Ru/C nanostructure labelled anti-CRP was successfully combined with CRP/anti-CRP/Au-COFs/ GCE (curve e).

Optimisation of method

Despite being immobilised successfully, the concentration of the antibody, incubation time of antigen (40 μg/mL) and incubation time of labelled antibody can directly affect the intensity of the signal. Thus, the following parameters were optimised: (a) antibody concentration; (b) CRP incubation time; (c) incubation time of labelled antibody. Respective text and figures on optimisations are given in the Electronic Supporting Material. In short, the following experimental conditions were found to give the best results: the anti-CRP concentration of 30 μg/mL (Fig. S3), the anti-CRP time with 60 min (Fig. S4) and antigen CRP incubation time with 60 min (Fig. S5). These values were chosen as optimised conditions.

Analytical performance

The relationship of the current with the concentration of CRP for the proposed immunosensor under optimal experimental conditions is illustrated in Fig. 5(a). The response current increased with the enhancement concentration of CPR (Fig. 5(b)). As can be seen, a good linear relationship between the logarithm concentration of CRP and the current response of the sensor was obtained, ranging from 0.2 to 20 ng/mL (Fig. 5(b)). The linear equation is I (μA) = 6.05 lgC (ng/mL) + 5.83. A detection limit of 0.1 ng/mL was also calculated by 3σ rule. Pt/Ru/C nanoparticles exhibited excellent catalytic behaviour toward small molecules of H_2O_2, and COFs have proved to have excellent conductivity, which promotes the sensitivity and extends the detection range. This sensitivity is comparable or better than that of some previous correlative works [3, 33–35] (Table 1).

To investigate the selectivity of immunosensor, under the optimised conditions, bovine serum albumin (BSA, 100 ng/mL), human chorionic gonadotrophin (HCG, 100 ng/mL), alanine (Ala, 100 ng/mL) and glycine (Gly, 100 ng/mL) were used to evaluate the selectivity of the immunosensor and compared with the response of 50 ng/mL of CRP. The results are collected in Fig. 5(c, d), indicating that the BSA, HCG, Gly and Ala did not cause any significant interference to the immunosensor according to the current. Therefore, it can be affirmed that the assay has a high selectivity toward CRP.

Table 1 Analytical performance of correlative methods for CRP detection

Methods applied	Materials used	Linear range	Detection limit	Reference	
Simultaneous photoelectrochemical immunoassay of dual cardiac markers using specific enzyme tags: a proof of principle for multiplexed bioanalysis	CdS quantum dots (QDs)/TiO_2 nanotubes	50 to 50 μg/mL	50 ng/mL	*Anal. Chem.*, 2016, 88, 1990–199-4	The alkaline phosphatase was employed to generate the signal. However, the limited stability of the immobilised enzyme and their native conformations could be easily disrupted by slight changes in the environment, which led to the loss of their catalytic activities.
On-chip determination of C-reactive protein using magnetic particles in continuous flow	Magnetic particles	1–10 μg/mL	0.87 μg/mL	*Anal. Chem.*, 2014, 86, 10552–10-559	The sensitivity was unsatisfactory
A pressure-based bioassay for the rapid, portable and quantitative detection of C-reactive protein	Magnetic particles and Pt particles	0.25 to 0.025 μg/-mL	0.2 ng/mL	*Chem. Commun.*, 2016, 52, 8452–845-4	A pressuremeter was not an accurate measuring instrument, which may cause huge standard deviation.
Ultrasensitive label-free immunoassay for C-reactive protein detection in human serum based on the electron transfer	Molybdenum disulphide–polyaniline–-gold nanoparticles	0.2−80 ng/mL	40 pg/mL	*Anal. Methods*, 2016, 6202–620-7	Turn-off mode design might cause false-positive signals.
Metal–organic frameworks nanomaterials as novel signal probes for electron transfer mediated ultrasensitive electrochemical immunoassay	Metal–organic frameworks nonmaterial	1–400 ng/mL	0.2 ng/mL	*Anal. Chem.*, 2016, 88, 12516–12-523	Although metal–organic frameworks nanomaterials (MOFs) conjugated protein was stable in water, MOFs themselves will be collapsed about few hours without gold nanoparticle conjugation.
Amperometric immunosensor based on covalent organic frameworks and Pt/Ru/C nanoparticles for the quantification of C-reactive protein	Pt/Ru/C nanoparticle	0.2–20 ng/mL	0.1 ng/mL	This work	The biosensor did not employ enzyme to generate the signal, which was highly stable and sensitive. And the Pt/Ru/C NPs were dispersed in water very well.

Repeatability, stability and reusability of the immunosensor

The intra-assay precision of the electrochemical CRP immunosensor was assessed via five reproduced measurements. The intra-assay variation coefficient was 4.0% at a concentration of 100 ng/mL of CRP, which show that this approach has excellent repeatability.

Stability is also an essential factor when the performance of the biosensor is evaluated. Therefore, the stability of the result of this electrode construction strategy was also investigated. The immunosensor could keep 90% of the initial response value after 1 mouth, demonstrating acceptable stability. The immunosensor for CRP could be regenerated through soaking with urea solution for 40 min, indicating that the immunosensor had excellent reusability.

Table 2 The recovery of CRP immunosensor

No.	Added (ng/mL)	Found (ng/mL)	RSD (%, $n = 3$)	Recovery (%)
1	5.0	5.033[a] ± 0.153[b]	3.3	100.7
2	10.0	10.20[a] ± 0.30[b]	3.3	102.0
3	30.0	28.80[a] ± 1.64[b]	5.6	96.0

[a]Mean value of four determinations

[b]Standard deviation

Recovery of the immunosensor

Standard addition method was used to prove the practicability of the proposed immunosensor. In this work, the serum samples were obtained from the Hospital of Yunnan Normal University (Kunming, China). Briefly, blood samples were centrifuged with 1000–1200 g (relative centrifugal force, RCF) for 5 min to get a serum sample. After being diluted to 10-fold with the buffer, three serum samples were mixed with CRP antigens standard solution to get final CRP concentration of 5, 10 and 30 ng/mL, respectively. Then, the immunosensor was incubated with different concentrations of CRP solutions for 50 min at 37 °C, followed by rinsing thoroughly with PBS and dried. Next, the immunosensor was incubated with 10 μL of Pt/Ru/C-labelled anti-CRP for 45 min at 37 °C. Afterwards, it was rewashed with PBS. Regarding the immunosensor as the working electrode, 100 μL of 1 mol/L H_2O_2 was added to10 mL of 0.1 mol/L PBS for the chronoamperometry determination at − 0.2 V to realise the quantitative determination of CRP. The recoveries at the concentrations of 5, 10 and 30 ng/mL were between 100.7 and 96% (see Table 2). The results are satisfactory, which indicates the assay can be applied to detect CRP in real samples.

Conclusions

In this paper, covalent organic frameworks material was used as the immobilisation matrix of C-reactive protein antibody to construct a novel and sensitive sandwich-type electrochemical immunosensor for the determination of C-reactive protein. Pt/Ru/C nanomaterials labelled on the antibody can directly catalyse the reduction of H_2O_2 in order to realise the successful determination of CRP and to enhance the sensitivity of immunosensors. This sensor has a good performance of response, high selectivity and a low detection limit (0.1 ng/mL). The major limitation is that the regeneration procedure through soaking with urea solution takes 40 min. The sensor can be applied to detect CRP in real samples with satisfactory results.

Funding information This work is supported by grants awarded by the National Natural Science Foundation of China (Grants 21465026, 21605130 and 21864026) and the Natural Science Foundation of Yunnan Province (Grants No. 2016FD017 and 2018FB016).

Compliance with ethical standards

Conflict of interest The authors declare that they have no competing interests.

References

1. Kim C, Ahn J, Kim J, Choi J, Lim K, Park TJ, Heo NS, Lee HG, Kim J, Choi Y (2013) CRP detection from serum for chip-based point-of-care testing system. Biosens Bioelectron 41:322–327
2. Hennessey H, Afara N, Omanovic S, Padjen AL (2009) Electrochemical investigations of the interaction of C-reactive protein (CRP) with a CRP antibody chemically immobilized on a gold surface. Anal Chim Acta 643:45–53
3. Liu T, Hu R, Zhang X, Zhang K, Liu Y, Zhang X, Bai R, Li D, Yang Y (2016) Metal-organic frameworks nanomaterials as novel signal probes for electron transfer mediated ultrasensitive electrochemical immunoassay. Anal Chem 88:12516–12523
4. Hermann M, Fischer D, Hoffmann MM, Gasser T, Quitzau K, Meinertz T, Münzel T, Lüscher TF (2012) CRP and CD14 polymorphisms correlate with coronary plaque volume in patients with coronary artery disease–IVUS substudy of the ENCORE trials. Atherosclerosis 220:172–176
5. Veeranna V, Zalawadiya SK, Niraj A, Kumar A, Ference B, Afonso L (2013) Association of novel biomarkers with future cardiovascular events is influenced by ethnicity: results from a multi-ethnic cohort. Int J Cardiol 166:487–493
6. May A, Wang TJ (2007) Evaluating the role of biomarkers for cardiovascular risk prediction: focus on CRP, BNP and urinary microalbumin. Expert Rev Mol Diagn 7:793–804
7. Mygind ND, Harutyunyan MJ, Mathiasen AB, Ripa RS, Thune JJ, Gøtze JP, Johansen JS, Kastrup J (2011) The influence of statin treatment on the inflammatory biomarkers YKL-40 and HsCRP in patients with stable coronary artery disease. Inflamm Res 60: 281–287
8. Yang T, Gao Y, Liu Z, Xu J, Lu L, Yu Y (2017) Three-dimensional gold nanoparticles/prussian blue-poly(3,4-ethylenedioxythiophene) nanocomposite as novel redox matrix for label-free electrochemical immunoassay of carcinoembryonic antigen. Sensors Actuators B Chem 239:76–84
9. Qian Y, Tang D, Du L, Zhang Y, Zhang L, Gao F (2015) A novel signal-on electrochemical DNA sensor based on target catalyzed hairpin assembly strategy. Biosens Bioelectron 64:177–181
10. Qian Y, Wang C, Gao F (2015) Ultrasensitive electrochemical detection of DNA based on Zn2+ assistant DNA recycling followed with hybridization chain reaction dual amplification. Biosens Bioelectron 63:425–431
11. Jia H, Yang T, Zuo Y, Wang W, Xu J, Lu L, Li P (2017) Immunosensor for α-fetoprotein based on a glassy carbon electrode modified with electrochemically deposited N-doped graphene, gold nanoparticles and chitosan. Microchim Acta 184:3747–3753
12. Zheng SS, Gu HZ, Yin DY, Zhang JL, Li W, Fu Y (2020) Biogenic synthesis of AuPd nanocluster as a peroxidase mimic and its application for colorimetric assay of acid phosphatase. Colloids Surf A Physicochem Eng Asp 589:124444
13. Scida K, Stege PW, Haby G, Messina GA, García CD (2011) Recent applications of carbon-based nanomaterials in analytical chemistry: critical review. Anal Chim Acta 69:16–17
14. Yang L, Liu X, Lu Q, Huang N, Liu M, Zhang Y, Yao S (2016) Catalytic and peroxidase-like activity of carbon based-Au Pd bimetallic nanocomposite produced using carbon dots as the reductant. Anal Chim Acta 930:23–30
15. Yang M, Zhang CH, Lv QT, Sun GH, Bi CL, Guo SX, Dong HX, Liu LJ (2020) Rational design of novel efficient palladium electrode embellished 3D hierarchical graphene/polyimide foam for hydrogen peroxide electroreduction. ACS Appl Mater Interfaces 12:934–944
16. Zhou Q, Wang W, Xiao J, Wang J, Liu G, Shi Q, Guo G (2006) Comparison of the enrichment efficiency of multiwalled carbon nanotubes, C18 silica, and activated carbon as the adsorbents for

the solid phase extraction of atrazine and simazine in water samples. Microchim Acta 152:215–224
17. Wu W, Li Y, Jin J, Wu H, Wang S, Ding Y, Ou J (2016) Sensing nitrite with a glassy carbon electrode modified with a three-dimensional network consisting of Ni_7S_6 and multi-walled carbon nanotubes. Microchim Acta 183:3159–3166
18. Dong H, Yu H, Wang X, Zhou Q, Feng J (2012) A novel structure of scalable air-cathode without nafion and Pt by rolling activated carbon and PTFE as catalyst layer in microbial fuel cells. Water Res 46:5777–5787
19. Zhang F, Pant D, Logan BE (2011) Long-term performance of activated carbon air cathodes with different diffusion layer porosities in microbial fuel cells. Biosens Bioelectron 30:49–55
20. Mahmood J, Li F, Jung S, Okyay MS, Ahmad I, Kim S, Park N, Jeong HY, Baek J (2017) An efficient and pH-universal ruthenium-based catalyst for the hydrogen evolution reaction. Nat Nanotech 12:441–446
21. Su J, Yang Y, Xia G, Chen J, Jiang P, Chen Q (2017) Ruthenium-cobalt nanoalloys encapsulated in nitrogen-doped graphene as active electrocatalysts for producing hydrogen in alkaline media. Nat Commun 8:14969
22. Xie Y, Tu XL, Ma X, Fang QW, Liu GB, Dai RY, Qu F, Yu YF, Lu LM, Huang XG (2019) A CuO-CeO_2 composite prepared by calcination of a bimetallic metal-organic framework for use in an enzyme-free electrochemical inhibition assay for malathion. Microchim Acta 186:567
23. Yang T, Yin L, He M, Wei W, Cao G, Ding X, Wang Y, Zhao Z, Yu T, Zhao H, Zhang D (2019) Yolk–shell hierarchical catalyst with tremella-like molybdenum sulfide on transition metal (Co, Ni and Fe) sulfide for electrochemical water splitting. Chem Commun 55: 14343–14346
24. Barman BK, Sarkar B, Nanda KK (2019) Pd-coated Ru nanocrystals supported on N-doped graphene as HER and ORR electrocatalysts. Chem Commun 55:13928–13931
25. Lukose B, Kuc A, Heine T (2011) The structure of layered covalent-organic frameworks. Chem Eur J 17:2388–2392
26. Chen L, Furukawa K, Gao J, Nagai A, Nakamura T, Dong Y, Jiang D (2014) Photoelectric covalent organic frameworks: converting open lattices into ordered donor-acceptor heterojunctions. J Am Chem Soc 136:9806–9809
27. Yaghi OM, Côté AP, Benin AI, Ockwig NW, O'Keeffe M, Matzger AJ (2005) Porous, crystalline, covalent organic frameworks. Science 310:1166–1170
28. Yang Z, Cao D (2012) Effect of Li doping on diffusion and separation of hydrogen and methane in covalent organic frameworks. J Phys Chem C 116:12591–12598
29. Ding X, Chen L, Honsho Y, Feng X, Saengsawang O, Guo J, Saeki A, Seki S, Irle S, Nagase S, Parasuk V, Jiang D (2011) An n-channel two-dimensional covalent organic framework. J Am Chem Soc 133:14510–14513
30. Wang W, Ding SY, Gao J, Wang Q, Zhang Y, Song WG, Su CY (2011) Construction of covalent organic framework for catalysis: Pd/COF-LZU1 in Suzuki–Miyaura coupling reaction. J Am Chem Soc 133:19816–19822
31. Das G, Biswal BP, Kandambeth S, Venkatesh V, Kaur G, Addicoat M, Heine T, Verma S, Banerjee R (2015) Chemical sensing in two dimensional porous covalent organic nanosheets. Chem Sci 6: 3931–3939
32. Qiu XL, Lu LM, Leng J, Yu YF, Wang WM, Jiang M, Ba L (2016) An enhanced electrochemical platform based on graphene oxide and multi-walled carbon nanotubes nanocomposite for sensitive determination of Sunset Yellow and Tartrazine. Food Chem 190: 889–895
33. Zhang N, Ma ZY, Ruan YF, Zhao WW, Xu JJ, Chen HY (2016) Simultaneous photoelectrochemical immunoassay of dual cardiac markers using specific enzyme tags: a proof of principle for multiplexed bioanalysis. Anal Chem 88:1990–1994
34. Matsuura R, Tawa K, Kitayama Y, Takeuchi T (2016) A plasmonic chip-based bio/chemical hybrid sensing system for the highly sensitive detection of C-reactive protein. Chem Commun 52:3883–3886
35. Zhang X, Hu R, Zhang K, Bai R, Li D, Yang Y (2016) Ultrasensitive label-free immunoassay for C-reactive protein detection in human serum based on the electron transfer. Anal Methods 8:6202–6207